DOI:10.12177/emca.2024.087　　文章编号:1673-6540(2024)09-0042-09　　中图分类号:TM 351　　文献标志码:A

# 一种永磁同步电机模型预测转矩控制简化策略研究

李耀华*, 种国臣, 郭伟超, 高　赛, 王钦政, 王自臣, 徐志雄
(长安大学 汽车学院,陕西 西安　710064)

# Study on a Simplified Strategy for Model Predictive Torque Control of Permanent Magnet Synchronous Motors

LI Yaohua*, CHONG Guochen, GUO Weichao, GAO Sai, WANG Qinzheng, WANG Zichen, XU Zhixiong
(School of Automotive, Chang'an University, Xi'an 710064, China)

**Abstract**: To address the issue of the heavy computational burden in traditional model predictive torque control (MPTC) for permanent magnet synchronous motors (PMSMs), a simplified MPTC strategy was proposed. By analyzing the utilization rates of basic voltage vectors in different stator flux linkage sectors, voltage vectors with lower utilization rates were discarded, thereby reducing the number of candidate voltage vectors. Additionally, the utilization of the zero-voltage vector under different absolute values of torque error was analyzed. When the torque error was small, the zero-voltage vector was directly applied; when the torque error was large, the zero-voltage vector was discarded, reducing the maximum number of candidate voltage vectors to four. Furthermore, a flux linkage error constraint was added to the cost function, effectively reducing flux linkage ripple. Simulation results showed that, compared to traditional MPTC, the proposed simplified control strategy effectively reduced the number of MPTC traversals, alleviated the computational burden, lowered the system's switching frequency, and maintained similar control performance.

**Key words**: permanent magnet synchronous motor; model predictive torque control; torque error; computational burden

**摘　要**: 针对永磁同步电机传统模型预测转矩控制(MPTC)在线计算负担较大的问题,提出了一种 MPTC 简化策略。通过分析基本电压矢量在定子磁链不同扇区的利用率,舍弃利用率较小的电压矢量,减小备选电压矢量数量。并分析不同转矩误差绝对值下的零电压矢量的利用率,当转矩误差较小时,直接输出零电压矢量;当转矩误差较大时,舍弃零电压矢量,将备选电压矢量最大数量减小至 4 个。进一步,通过成本函数增加磁链误差约束,有效降低磁链脉动。仿真结果表明,与传统 MPTC 相比,所提简化控制策略可有效减少 MPTC 系统遍历次数,减轻计算负担,降低系统开关频率,且控制性能基本相当。

**关键词**: 永磁同步电机; 模型预测转矩控制; 转矩误差; 计算负担

**基金项目**: 西安市碑林区科技计划项目(GX2252)
Xi'an Beilin District Science and Technology Program (GX2252)

## 0　引言

模型预测控制(Model Predictive Control, MPC)因其性能优越、结构简单以及灵活性好,在永磁同步电机(Permanent Magnet Synchronous Motor,PMSM)控制领域受到广泛关注[1-8]。传统有限控制集模型预测控制(Finite Control Set-MPC, FCS-MPC)在预测过程中需要枚举所有基本电压矢量进行计算,计算负担较大。因此,简化计算量和提高实时性成为 MPC 的重要问题。文献[9]从简化预测模型出发减小计算工作量,但依然采用全部备选电压矢量。文献[10-13]从提升硬件出发,采用现场可编程逻辑门阵列(Field Programmable Gate Array,FPGA)和多核处理器提升实时性,但增加了硬件成本。文献[14-16]基于当前时刻开关状态舍弃开关次数较多的备选电压矢量,可减小开关次数,但会恶化控制性能。文献[17]通过评估三个不相邻的有效电压矢量,确定两个相邻最优有效电压矢量,减少预测计算量。文献[18-19]将备选电压矢量减小为直接转矩控

制选择的电压矢量与零电压矢量。文献[20]基于转矩误差大小备选电压矢量集合选择零电压矢量或非零电压矢量,将最大备选电压矢量数目减小至 6 个。文献[21]通过增加约束舍弃利用率较低的电压矢量。

本文基于表贴式永磁同步电机(Surface-Mounted PMSM, SPMSM)模型预测转矩控制(Model Predictive Torque Control, MPTC)模型,通过磁链扇区约束,将备选电压矢量数量降至 5 个,并增加转矩脉动约束,进一步减小备选电压矢量数量至 4 个。并在此基础上,通过成本函数增加磁链误差约束,有效降低磁链脉动。仿真结果表明,与传统 MPTC 策略相比,简化后的控制策略可有效减少 MPTC 系统遍历次数,减轻计算负担,降低系统开关频率,且控制性能基本相当。

## 1 永磁同步电机模型预测转矩控制

定子磁链坐标系下,施加电压矢量一个采样周期后,定子磁链变化情况如图 1 所示。

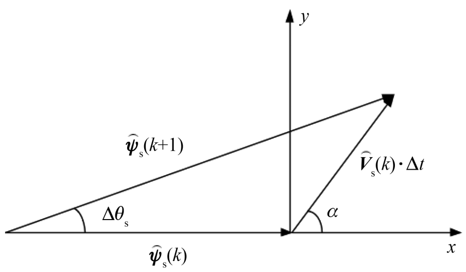


**图 1 定子磁链变化**

**Fig. 1 Changes in stator flux linkage**

图 1 中:$\hat{\psi}_s$、$\delta$ 和 $T_e$ 分别为定子磁链、转矩角和转矩实际值;$k$ 和 $k+1$ 分别为当前时刻和下一时刻;$\hat{V}_s$ 为电压矢量幅值;$\alpha$ 为定子磁链与电压矢量的夹角;$\Delta\theta_s$ 为定子磁链角变化量;$\Delta t$ 为系统采样时间。由图 1 可知,下一时刻的 SPMSM 定子磁链、转矩角和转矩如式(1)~式(3)所示[22]:

$$\begin{cases}\hat{\psi}_s(k+1)=\hat{\psi}_s(k)\sqrt{1+q^2+2q\cos\alpha}\\ q=\dfrac{\hat{V}_s(k)\cdot\Delta t}{\hat{\psi}_s(k)}\end{cases}\tag{1}$$

$$\delta(k+1)\approx\delta(k)+\Delta\theta_s=\delta(k)+\arcsin\left(\frac{q\sin\alpha}{\sqrt{1+q^2+2q\cos\alpha}}\right)\tag{2}$$

$$T_e(k+1)=\frac{3p\hat{\psi}_s(k+1)\psi_f}{2L_d}\sin[\delta(k+1)]\tag{3}$$

式中:$p$ 为电机极对数;$L_d$ 为 $d$ 轴电感;$\psi_f$ 为永磁体磁链。

按开关次数最小原则来选取开关状态 000 或 111 生成零矢量[23],备选电压矢量集合如式(4)所示:

$$\boldsymbol{V}_s\in\{\boldsymbol{V}_0,\boldsymbol{V}_1,\boldsymbol{V}_2,\boldsymbol{V}_3,\boldsymbol{V}_4,\boldsymbol{V}_5,\boldsymbol{V}_6\}\tag{4}$$

定义成本函数如式(5)所示[24]:

$$g=\sqrt{\left(\frac{T_e(k+1)-T_e^*}{T_e^*}\right)^2+\left(\frac{\hat{\psi}_s(k+1)-\hat{\psi}_s^*}{\hat{\psi}_s^*}\right)^2}\tag{5}$$

式中:$T_e^*$ 和 $\hat{\psi}_s^*$ 分别为转矩和定子磁链参考值。

传统 MPTC 系统框图如图 2 所示。基于 Matlab/Simulink 构建 SPMSM MPTC 模型并进行仿真。仿真中,采样频率为 20 kHz、$K_p=5$ 且 $K_i=10$。参考转速在 2 s 时由初始 80 rpm 阶跃至 −80 rpm;负载转矩在 1 s 时由初始 10 N·m 阶跃

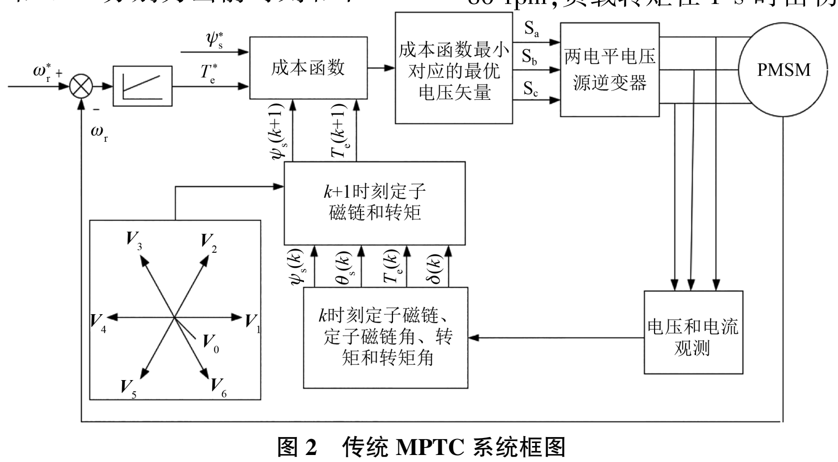


**图 2 传统 MPTC 系统框图**

**Fig. 2 Block diagram of traditional MPTC system**

至-10 N·m,在 3 s 时再次阶跃至 10 N·m,运行总时长为 4 s。仿真系统参数如表 1 所示。仿真结果如图 3~图 5 所示。

**表 1 仿真系统参数**

**Tab. 1 Parameters of simulation system**

| 参数名称 | 参数值 |
|---|---|
| 直流母线电压 $U_{dc}$/V | 312 |
| 定子电阻 $R_s$/Ω | 0.2 |
| 转子磁链 $\psi_f$/Wb | 0.175 |
| $d$ 轴电感 $L_d$/H | 0.008 5 |
| $q$ 轴电感 $L_q$/H | 0.008 5 |
| 极对数 $p$ | 4 |

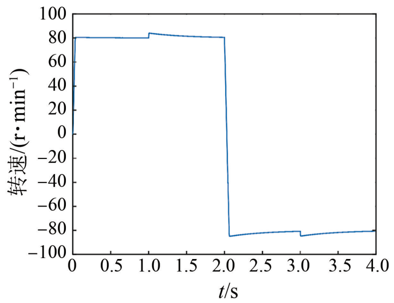


**图 3 传统 MPTC 下的 SPMSM 转速**

**Fig. 3 Speed of SPMSM under traditional MPTC**

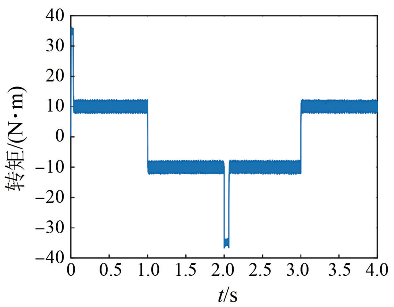


**图 4 传统 MPTC 下的 SPMSM 转矩**

**Fig. 4 Torque of SPMSM under traditional MPTC**

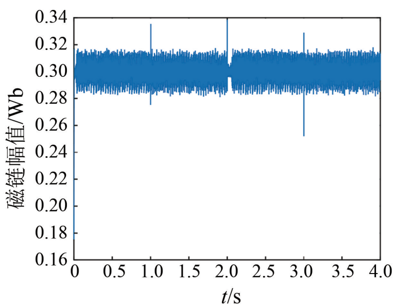


**图 5 传统 MPTC 下的 SPMSM 定子磁链**

**Fig. 5 Stator flux linkage of SPMSM under traditional MPTC**

定义转矩脉动均方根误差(Root Mean Square Error,RMSE)、磁链脉动 RMSE 和平均开关频率分别如式(6)~式(8)所示:

$$T_{rip\_RMSE} = \sqrt{\frac{\sum_{i=1}^{n}(T_e - T_e^*)^2}{n}} \tag{6}$$

$$\psi_{rip\_RMSE} = \sqrt{\frac{\sum_{i=1}^{n}(\psi_s - \psi_s^*)^2}{n}} \tag{7}$$

$$f_{ave} = \frac{N_{switching}}{6t} \tag{8}$$

式中:$n$ 为采样点数;$N_{switching}$ 为逆变器上下桥臂总开关次数;$t$ 为仿真总时长。

综合图 3~图 5 以及式(6)~式(8),得到传统 MPTC 性能如表 2 所示。

**表 2 传统 MPTC 性能**

**Tab. 2 Performance of traditional MPTC**

| 参数名称 | 参数值 |
|---|---|
| $T_{rip\_RMSE}$/(N·m) | 1.171 3 |
| $\psi_{rip\_RMSE}$/Wb | 0.005 3 |
| $f_{ave}$/kHz | 6.55 |

## 2 磁链扇区约束

定义电压矢量利用率如式(9)所示:

$$\eta_{V_i} = \frac{N_{V_i}}{N_{total}} \times 100\% \tag{9}$$

式中:$\eta_{V_i}$ 为电压矢量利用率,$i=0,1\cdots,6$;$N_{V_i}$ 为电压矢量选择数量;$N_{total}$ 为电压矢量总体数量。

以上文仿真结果为例,当定子磁链位于 $\theta_1$ 扇区,MPTC 共施加 12 509 个电压矢量。其中,选择 $\boldsymbol{V}_0$ 共 4 256 次,占比 34.02%;选择 $\boldsymbol{V}_1$ 共 837 次,占比 6.69%;选择 $\boldsymbol{V}_2$ 共 1 661 次,占比 13.28%;选择 $\boldsymbol{V}_3$ 共 1 653 次,占比 13.21%;选择 $\boldsymbol{V}_4$ 共 800 次,占比 6.40%;选择 $\boldsymbol{V}_5$ 共 1 588 次,占比 12.69%;选择 $\boldsymbol{V}_6$ 共 1 714 次,占比 13.70%。同理可得其他扇区数据,如表 3 所示。

由表 3 可知,在每个扇区,MPTC 选择电压矢量并不均衡,不同电压矢量在每个扇区内的利用率有较大差异。因此,可将每个扇区利用率较低的两个电压矢量舍弃,即 $\theta_1$ 和 $\theta_4$ 扇区舍弃 $\boldsymbol{V}_1$ 和 $\boldsymbol{V}_4$,$\theta_2$ 和 $\theta_5$ 扇区舍弃 $\boldsymbol{V}_2$ 和 $\boldsymbol{V}_5$,$\theta_3$ 和 $\theta_6$ 扇区舍弃 $\boldsymbol{V}_3$ 和 $\boldsymbol{V}_6$,从而将备选电压矢量数量由 7 个降为 5 个,减小计算负担。

表 3 电压矢量利用率

Tab. 3 Voltage vector utilization rates %

| 电压矢量 | 利用率 | | | | | |
| --- | --- | --- | --- | --- | --- | --- |
| | $\theta_1$ | $\theta_2$ | $\theta_3$ | $\theta_4$ | $\theta_5$ | $\theta_6$ |
| $V_0$ | 34.02 | 34.54 | 32.74 | 34.98 | 33.84 | 34.86 |
| $V_1$ | 6.69 | 13.43 | 13.74 | 6.23 | 12.34 | 12.92 |
| $V_2$ | 13.28 | 6.48 | 13.60 | 13.12 | 6.26 | 13.01 |
| $V_3$ | 13.21 | 13.40 | 6.55 | 13.05 | 13.96 | 6.39 |
| $V_4$ | 6.40 | 13.39 | 13.98 | 6.38 | 12.97 | 12.46 |
| $V_5$ | 12.69 | 5.98 | 13.25 | 13.75 | 6.62 | 13.48 |
| $V_6$ | 13.70 | 12.78 | 6.14 | 12.48 | 14.00 | 6.89 |

相同仿真条件下，考虑磁链扇区约束的 SPSMSM MPTC 仿真结果如图 6～图 8 所示。

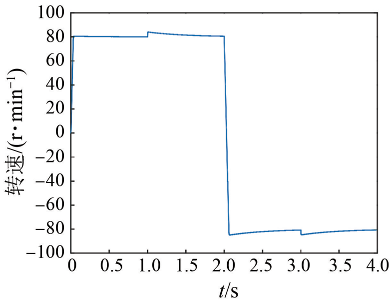


图 6 考虑磁链扇区约束的 SPMSM 转速

Fig. 6 Speed of SPMSM considering flux sector constraint

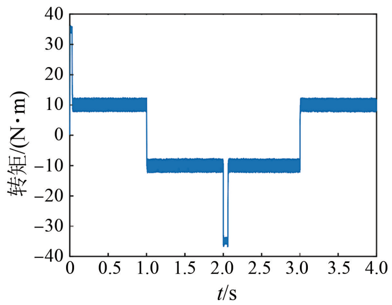


图 7 考虑磁链扇区约束的 SPMSM 转矩

Fig. 7 Torque of SPMSM considering flux sector constraint

相同仿真条件下，考虑磁链扇区约束的 MPTC 性能如表 4 所示。

表 4 考虑磁链扇区约束的 MPTC 性能

Tab. 4 Performance of MPTC considering flux sector constraint

| 参数名称 | 参数值 |
| --- | --- |
| $T_{rip\_RMSE}$/(N·m) | 1.232 6 |
| $\psi_{rip\_RMSE}$/Wb | 0.006 0 |
| $f_{ave}$/kHz | 6.46 |

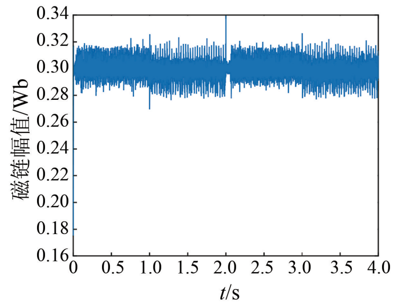


图 8 考虑磁链扇区约束的 SPMSM 定子磁链

Fig. 8 Stator flux linkage of SPMSM considering flux sector constraint

考虑磁链扇区约束的 MPTC 备选电压矢量数量减小至 5 个，由表 4 可知，相较于传统 MPTC，$T_{rip\_RMSE}$ 增大 5.15%，$\psi_{rip\_RMSE}$ 增大 13.21%，$f_{ave}$ 减小 1.37%，可见控制性能基本相当。

## 3 磁链扇区和转矩误差约束

由于零电压矢量缓慢减小磁链和转矩，当转矩脉动较小时，MPTC 更多选择零电压矢量；当转矩脉动较大时，MPTC 更多选择非零电压矢量。考虑磁链扇区约束的 MPTC 在不同转矩误差范围内的零电压矢量选择情况如表 5 所示。

表 5 不同转矩误差范围的零电压矢量占比

Tab. 5 Percentage of zero-voltage vector in different torque error ranges

| $\lvert\Delta T_e\rvert$/(N·m) | $N_{total}$ | $N_{V_0}$ | 零矢量占比/% |
| --- | --- | --- | --- |
| [0, 0.1] | 4 957 | 3 742 | 75.49 |
| [0.1, 0.2] | 4 886 | 3 905 | 79.92 |
| [0.2, 0.3] | 4 929 | 4 098 | 83.14 |
| [0.3, 0.4] | 4 454 | 3 710 | 83.30 |
| [0.4, 0.5] | 4 137 | 3 401 | 82.21 |
| [0.5, 0.6] | 3 737 | 2 710 | 72.52 |
| [0.6, 0.7] | 3 239 | 2 103 | 64.93 |
| [0.7, 0.8] | 3 420 | 1 847 | 54.01 |
| [0.8, 0.9] | 3 679 | 1 045 | 28.40 |
| [0.9, 1.0] | 3 780 | 477 | 12.62 |
| [1.0, 1.1] | 4 080 | 152 | 3.73 |
| [1.1, 1.2] | 4 272 | 37 | 0.87 |
| [1.2, 1.3] | 4 485 | 15 | 0.33 |
| [1.3, 1.4] | 4 486 | 2 | 0.04 |
| [1.4, 1.5] | 4 448 | 1 | 0.02 |
| >1.5 | 17 011 | 1 | 0.005 |

由表 5 可知，当转矩误差绝对值为 0 N·m～0.8 N·m 时，零电压矢量使用率达到 75.58%；当转矩误差绝对值大于 0.8 N·m 时，零电压矢量使

用率仅为 3.74%。因此,当转矩误差绝对值为 0 N·m~0.8 N·m 时,电机系统直接输出零电压矢量;当转矩误差绝对值大于 0.8 N·m 时,将备选电压矢量集合中的零电压矢量舍弃,从而备选电压矢量最大数量减小为 4 个。

相同仿真条件下,考虑磁链扇区和转矩误差约束的 SPMSM MPTC 仿真结果如图 9~图 11 所示。

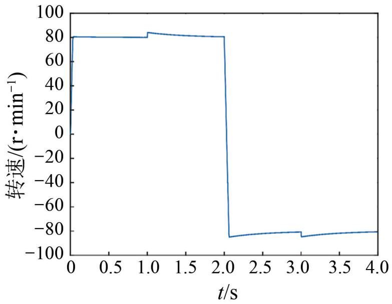


图 9　考虑磁链扇区和转矩误差约束的 SPMSM 转速

Fig. 9　Speed of SPMSM considering flux sector and torque error constraints

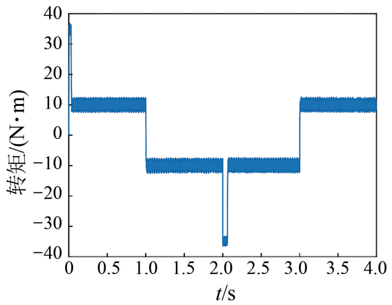


图 10　考虑磁链扇区和转矩误差约束的 SPMSM 转矩

Fig. 10　Torque of SPMSM considering flux sector and torque error constraints

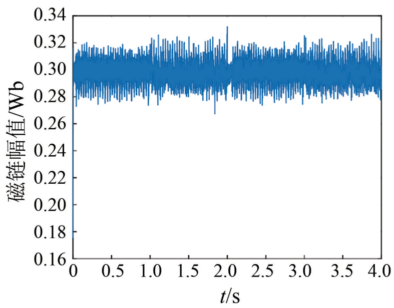


图 11　考虑磁链扇区和转矩误差约束的 SPMSM 定子磁链

Fig. 11　Stator flux linkage of SPMSM considering flux sector and torque error constraints

相同仿真条件下,考虑磁链扇区和转矩误差约束的 MPTC 性能如表 6 所示。

表 6　考虑磁链扇区和转矩误差约束的 MPTC 性能

Tab. 6　Performance of MPTC considering flux sector and torque error constraints

| 参数名称 | 参数值 |
|---|---|
| $T_{\mathrm{rip\_RMSE}}$/(N·m) | 1.178 4 |
| $\psi_{\mathrm{rip\_RMSE}}$/Wb | 0.007 4 |
| $f_{\mathrm{ave}}$/kHz | 4.36 |

由表 6 可知,考虑磁链扇区和转矩误差约束的 MPTC 将备选电压矢量数量减小至 4,提高了实时性能。相较于传统 MPTC,$T_{\mathrm{rip\_RMSE}}$ 增大 0.61%,$f_{\mathrm{ave}}$ 减小 33.44%,但 $\psi_{\mathrm{rip\_RMSE}}$ 增大 39.62%,可见控制性能较差。

## 4　增加磁链误差约束

由上文可知,增加磁链扇区和转矩误差约束后,相比于传统 MPTC,转矩脉动基本一致,但磁链脉动增大 39.62%。因此,可在成本函数中增加磁链误差约束项,以降低磁链脉动[25]。增加磁链误差约束项的成本函数如式(10)所示:

$$g = \sqrt{\left[\frac{T_e(k+1) - T_e^*}{T_e^*}\right]^2 + \left[\frac{\hat{\psi}_s(k+1) - \hat{\psi}_s^*}{\hat{\psi}_s^*}\right]^2} + g_f \tag{10}$$

$$g_f = \begin{cases} 10\,000, & |\hat{\psi}_s(k+1) - \hat{\psi}_s^*| > 0.01 \\ 0, & |\hat{\psi}_s(k+1) - \hat{\psi}_s^*| \leqslant 0.01 \end{cases} \tag{11}$$

式中:$g_f$ 为磁链误差约束函数。

相同仿真条件下,增加磁链误差约束的 SPMSM MPTC 仿真结果如图 12~图 14 所示。

相同仿真条件下,增加磁链误差约束的 MPTC 性能如表 7 所示。

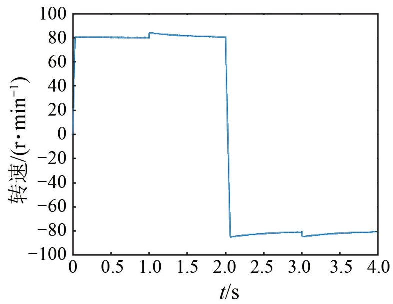


图 12　增加磁链误差约束的 SPMSM 转速

Fig. 12　Speed of SPMSM with increased flux error constraint

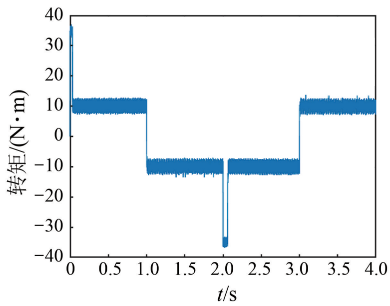


**图 13 增加磁链误差约束的的 SPMSM 转矩**

**Fig. 13 Torque of SPMSM with increased flux error constraint**

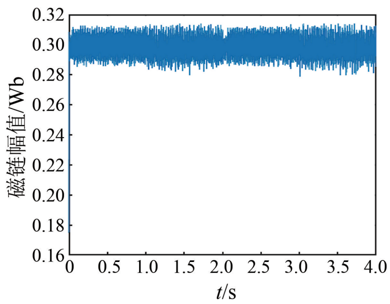


**图 14 增加磁链误差约束的 SPMSM 定子磁链**

**Fig. 14 Stator flux linkage of SPMSM with increased flux error constraint**

**表 7 增加磁链误差约束的 MPTC 性能**

**Tab. 7 Performance of MPTC with increased flux error constraint**

| 参数名称 | 参数值 |
|---|---|
| $T_{\mathrm{rip\_RMSE}}$/(N·m) | 1.166 9 |
| $\psi_{\mathrm{rip\_RMSE}}$/Wb | 0.005 8 |
| $f_{\mathrm{ave}}$/kHz | 4.15 |

不同控制策略性能对比如表 8 所示,其中 $N_{V_{\mathrm{s\_max}}}$ 为备选电压矢量的最大数量。

**表 8 不同控制策略性能**

**Tab. 8 Performance of different control strategies**

| 控制策略 | $T_{\mathrm{rip\_RMSE}}$/(N·m) | $\psi_{\mathrm{rip\_RMSE}}$/Wb | $f_{\mathrm{ave}}$/kHz | $N_{V_{\mathrm{s\_max}}}$ |
|---|---|---|---|---|
| 传统 MPTC | 1.171 3 | 0.005 3 | 6.55 | 7 |
| 磁链扇区约束 | 1.232 6 | 0.006 0 | 6.46 | 5 |
| 磁链扇区和转矩误差约束 | 1.178 4 | 0.007 4 | 4.36 | 4 |
| 增加磁链误差约束 | 1.166 9 | 0.005 8 | 4.15 | 4 |

由表 8 可知,通过增加磁链误差约束,可有效减小磁链脉动。相较于传统 MPTC,$T_{\mathrm{rip\_RMSE}}$ 减小 0.38%,$\psi_{\mathrm{rip\_RMSE}}$ 增大 9.4%,可见,控制性能基本相当,但备选电压矢量的最大数量减小至 4,减轻了系统计算负担。

经统计,传统 MPTC 零电压矢量利用率为 34.49%;考虑磁链扇区约束的 MPTC 零电压矢量利用率为 34.08%;考虑磁链扇区和转矩误差约束的 MPTC 零电压矢量利用率为 51.55%;增加磁链误差约束的 MPTC 零电压矢量利用率为 53.99%,且开关频率较大降低,相较于传统 MPTC,开关频率降低 36.64%。

## 5 结语

(1) 通过磁链扇区约束,可将备选集合中的电压矢量数量降至 5 个。相较于传统 MPTC,转矩脉动 RMSE 增大 5.15%,磁链脉动 RMSE 增大 13.21%,开关频率减小 1.37%,控制性能基本相当。

(2) 通过磁链扇区和转矩误差约束,可将备选电压矢量最大数量减小至 4。相较于传统 MPTC,转矩脉动 RMSE 增大 0.61%,磁链脉动 RMSE 增大 39.62%,开关频率降低 33.44%,控制性能较差。

(3) 通过在成本函数中增加磁链误差约束项,可有效减小磁链脉动。相较于传统 MPTC,转矩脉动 RMSE 减小 0.38%,磁链脉动 RMSE 增大 9.4%,控制性能基本相当,但备选电压矢量数量减小至 4,减轻了系统计算负担。同时,由于零矢量利用率增大,使得开关频率降低 36.64%。

## 参 考 文 献

[1] RODRIGUEZ J, GARICA C, MORA A, et al. Latest advances of model predictive control in electrical drives-part I: Basic concepts and advanced strategies [J]. IEEE Transactions on Power Electronics, 2022, 37(4): 3927-3941.

[2] J RODRIGUEZ J, GARICA C, MORA A, et al. Latest advances of model predictive control in electrical drives-part II: Applications and benchmarking with classical control methods [J]. IEEE Transactions on Power Electronics, 2022, 37(5): 5047-5061.

[3] KARAMANAKOS P, GEYER T. Guidelines for the design of finite control set model predictive controllers [J]. IEEE Transactions on Power Electronics, 2020, 35(7): 7434-7450.

[4] LI T, SUN X D, LEI G, et al. Finite-control-set

model predictive control of permanent magnet synchronous motor drive systems-an overview [J]. IEEE/CAA Journal of Automatica Sinica, 2022, 9 (12): 2087-2105.

[5] 王治国, 郑泽东, 李永东,等. 交流电机模型预测控制综述[J]. 电机与控制学报, 2022, 26(11): 14-30.
WANG Z G, ZHENG Z D, LI Y D, et al. A review of model predictive control for AC motor [J]. Electric Machines and Control, 2022, 26(11): 14-30.

[6] 齐昕, 苏涛, 周珂, 等. 交流电机模型预测控制策略发展概述[J]. 中国电机工程学报, 2021, 41 (18): 6408-6418.
QI X, SU T, ZHOU K, et al. Development of AC motor model predictive control strategy: An overview [J]. proceedings of the CSEE, 2021, 41 (18): 6408-6418.

[7] 朱芮, 吴迪, 陈继峰, 等. 电机系统模型预测控制研究综述[J]. 电机与控制应用, 2019,46 (8): 1-10+30.
ZHU R, WU D, CHEN J F, et al. A review of research on motor system model predictive control [J]. Electric Machines & Control Application, 2019, 46(8): 1-10+30.

[8] 常勇, 包广清, 杨梅, 等. 模型预测控制在永磁同步电机系统中的应用发展综述[J]. 电机与控制应用, 2019, 46(8): 11-17.
CHANG Y, BAO G Q, YANG M, et al. Application and development of model predictive control in permanent magnet synchronous motor system [J]. Electric Machines & Control Application, 2019, 46 (8): 11-17.

[9] 李耀华, 师浩浩, 孟祥臻. 表面式永磁同步电机直接转矩控制系统简化预测控制策略[J]. 电机与控制学报, 2020, 24(4): 96-103.
LI Y H, SHI H H, MENG X Z. Simplified predictive control for direct torque control of surface permanent magnet synchronous motor [J]. Electric Machines and Control, 2020, 24(4): 96-103.

[10] GULBUDAK O, SANTI E. FPGA-based model predictive controller for direct matrix converter [J]. IEEE Transactions on Industrial Electronics, 2016, 63(7): 4560-4570.

[11] YANG C Y, LIU K, HU M J, et al. FPGA-based extended control set model predictive current control with a simplified search strategy for permanent magnet synchronous motor [J]. Electronics, 2023, 12: 4726.

[12] 刘涛, 习金生, 宋战锋, 等. 基于多核并行计算的永磁同步电机有限集模型预测控制策略[J]. 电工技术学报, 2021, 36(1): 107-119.
LIU T, XI J S, SONG Z F, et al. Finite control set model predictive control of permanent magnet synchronous motor based on multi-core parallel computing [J]. Transactions of China Electrotechnical Society, 2021, 36(1): 107-119.

[13] 齐昕, 吴文昊, 吴琳, 等. 基于时间辅助信息的感应电机预测电流控制[J]. 中国电机工程学报, 2019, 36(16): 4927-4934.
QI X, WU W H, WU L, et al. Predictive current control of induction machines based on time auxiliary information [J]. Proceeding of the CSEE, 2019, 36 (16): 4927-4934.

[14] 王伟光, 李伟. 基于 MTPA 的永磁同步电机模型预测转矩控制[J]. 电气传动, 2014, 44(11): 3-6.
WANG W G, LI W. Model predictive torque control method of permanent magnet synchronous motor based on MTPA [J]. Electric Drive, 2014, 44(11): 3-6.

[15] 周雅夫, 张霖, 王翰涛, 等. 车用永磁同步电机 FCS-MPC 方法研究[J]. 电力电子技术, 2019, 53 (1): 42-45.
ZHOU Y F, ZHANG L, WANG H T, et al. Research on FCS-MPC method of permanent magnet synchronous motor for vehicle [J]. Power Electronics, 2019, 53(1): 42-45.

[16] 李耀华, 刘子焜, 刘东梅, 等. 永磁同步电机直接转矩控制与模型预测转矩控制比较研究[J]. 电机与控制应用, 2021, 48(7): 18-25.
LI Y H, LIU Z K, LIU D M, et al. Comparison between DTC and MPTC for PMSM [J]. Electric Machines & Control Application, 2021, 48(7): 18-25.

[17] 杨狂彪, 陈鼎新, 石坚. 低复杂度永磁同步电机双矢量模型预测控制策略[J]. 电机与控制应用, 2024, 51(1): 87-96.
YANG K B, CHEN D X, SHI J. Low complexity dual vector model predictive control strategy for permanent magnet synchronous motor [J]. Electric Machines & Control Application, 2024, 51(1): 87-96.

[18] 李耀华, 赵承辉, 秦玉贵, 等. DTC 与 MPTC 自适

应切换的表贴式永磁同步电机控制策略[J]. 电机与控制应用, 2020, 47(2): 9-13.
LI Y H, ZHAO C H, QIN Y G, et al. Control strategy of adaptive switching between DTC and MPTC for surface permanent magnet synchronous motor [J]. Electric Machines & Control Application, 2020, 47(2): 9-13.

[19] HABIBULLAH M, LU D D, XIAO D, et al. A simplified finite-state predictive direct torque control for induction motor drive [J]. IEEE Transactions on Industrial Electronics, 2016, 63(8): 3964-3975.

[20] 李耀华, 曲亚飞, 刘子焜, 等. 基于转矩误差带的表贴式永磁同步电机 MPTC 系统精简策略[J]. 电机与控制应用, 2020, 47(12): 25-31.
LI Y H, QU Y F, LIU Z K, et al. Simplified control strategy for SPMSM MPTC system based on band of torque error [J]. Electric Machines & Control Application, 2020, 47(12): 25-31.

[21] 李耀华, 杨启东, 苏锦仕, 等. 基于电压矢量利用率的永磁同步电机模型预测转矩控制备选电压矢量集合[J]. 电机与控制应用, 2020, 47(4):10-17.
LI Y H, YANG Q D, SUN J S, et al. Candidate voltage vector sets used in model predictive torque control of permanent magnet synchronous motor based on utilization rate of voltage vectors [J]. Electric Machines & Control Application, 2020, 47(4): 10-17.

[22] 李耀华, 陈桂鑫, 王孝宇, 等. 表贴式永磁同步电机模型预测转矩控制预测模型研究[J]. 电机与控制应用, 2022, 49(1):16-21.
LI Y H, CHEN G Y, WANG X Y, et al. Research on predictive model of the SPMSM MPTC system [J]. Electric Machines & Control Application, 2022, 49(1):16-21.

[23] 李耀华, 杨启东, 曲亚飞, 等. 自适应变电压矢量 PMSM 直接转矩控制开关表[J]. 电机与控制学报, 2019, 23(9): 75-83.
LI Y H, YANG Q D, QU Y F, et al. Adaptive variable voltage vectors switching table in direct torque control for PMSM [J]. Electric Machines and Control, 2019, 23(9): 75-83.

[24] 李耀华, 刘洋, 孟祥臻. 一种表面式永磁同步电机有限状态集模型预测直接转矩控制[J]. 电机与控制学报, 2020, 24(8): 33-43.
LI Y H, LIU Y, MENG X Z. Finite control set model predictive direct torque control of surface permanent magnet synchronous motor [J]. Electric Machines and Control, 2020, 24(8): 33-43.

[25] 李耀华, 秦辉, 苏锦仕, 等. 表贴式永磁同步电机有限集模型预测转矩控制成本函数研究[J]. 电机与控制应用, 2019, 46(9): 12-18.
LI Y H, QIN H, SU J S, et al. Cost function of finite control set model predictive torque control of surface permanent magnet synchronous motor [J]. Electric Machines & Control Application, 2019, 46(9): 12-18.

收稿日期:2024-04-12
收到修改稿日期:2024-06-04

作者简介:
李耀华(1980-),男,博士,副教授,研究方向为电机电控与新能源汽车技术,nuaaliyaohua@ 126.com;
*通信作者:李耀华(1980-),男,博士,副教授,研究方向为电机电控与新能源汽车技术,nuaaliyaohua@ 126.com。

DOI: 10.12177/emca.2024.087

# Study on a Simplified Strategy for Model Predictive Torque Control of Permanent Magnet Synchronous Motors

LI Yaohua*, CHONG Guochen, GUO Weichao, GAO Sai, WANG Qinzheng, WANG Zichen, XU Zhixiong

(School of Automotive, Chang'an University, Xi'an 710064, China)

**Key words**: permanent magnet synchronous motor; model predictive torque control; torque error; computational burden

Model predictive control (MPC) has garnered widespread attention in the field of permanent magnet synchronous motor (PMSM) control due to its superior performance, simple structure, and good flexibility. Traditional finite control set model predictive control (FCS-MPC) requires enumerating all basic voltage vectors during the prediction process, resulting in a heavy computational burden. Therefore, simplifying the computation and improving real-time performance have become key issues in MPC.

Based on the model predictive torque control (MPTC) model for surface-mounted PMSMs, this paper proposes a simplified MPTC strategy. By analyzing the utilization rates of basic voltage vectors in different stator flux linkage sectors, voltage vectors with low utilization rates were discarded, reducing the number of candidate voltage vectors. Additionally, the utilization of the zero-voltage vector under different absolute values of torque error was analyzed. When the torque error was small, the zero-voltage vector was directly applied; when the torque error was large, the zero-voltage vector was discarded, reducing the maximum number of candidate voltage vectors to four. On this basis, a flux linkage error constraint was added to the cost function, effectively reducing flux linkage ripple. Simulation results showed that, compared to traditional MPTC, the proposed simplified strategy reduced the maximum traversal count of the MPTC system, lowered the system's average switching frequency, and maintained similar control performance.

The conclusions are as follows:

1. By applying flux linkage sector constraints, the number of voltage vectors in the candidate set could be reduced to five. Compared to traditional MPTC, the root mean square error (RMSE) of torque ripple increased by 5.15%, the RMSE of flux linkage ripple increased by 13.21%, the switching frequency decreased by 1.37%, and the control performance remained comparable.

2. By applying both flux linkage sector constraints and torque error constraints, the maximum number of candidate voltage vectors could be reduced to four. Compared to traditional MPTC, the RMSE of torque ripple increased by 0.61%, the RMSE of flux linkage ripple increased by 39.62%, and the switching frequency decreased by 33.44%, resulting in reduced control performance.

3. By adding a flux linkage error constraint term to the cost function, flux linkage ripple could be effectively reduced. Compared to traditional MPTC, the RMSE of torque ripple decreased by 0.38%, the RMSE of flux linkage ripple increased by 9.4%, and the control performance remained comparable. At the same time, the number of candidate voltage vectors was reduced to four, alleviating the computational burden on the system, while the increased utilization of the zero-voltage vector reduced the switching frequency by 36.64%.